rec'd
2/16/71

NASA TECHNICAL NOTE

NASA TN D-6146

NASA TN D-6146

LAMINATION RESIDUAL STRESSES IN MULTILAYERED FIBER COMPOSITES

by Christos C. Chamis

Lewis Research Center

Cleveland, Ohio 44135

NATIONAL AERONAUTICS AND SPACE ADMINISTRATION • WASHINGTON, D. C. • FEBRUARY 1971

1. Report No. NASA TN D-6146	2. Government Accession No.	3. Recipient's Catalog No.
4. Title and Subtitle LAMINATION RESIDUAL STRESSES IN MULTILAYERED FIBER COMPOSITES		5. Report Date February 1971
		6. Performing Organization Code
7. Author(s) Christos C. Chamis		8. Performing Organization Report No. E-5848
		10. Work Unit No. 129-03
9. Performing Organization Name and Address Lewis Research Center National Aeronautics and Space Administration Cleveland, Ohio 44135		11. Contract or Grant No.
		13. Type of Report and Period Covered Technical Note
12. Sponsoring Agency Name and Address National Aeronautics and Space Administration Washington, D. C. 20546		14. Sponsoring Agency Code
15. Supplementary Notes		

16. Abstract

Residual stresses arising from the lamination fabrication process are investigated using linear laminate theory. An equation to predict the residual stresses is given. The pertinent variables that influence residual stresses are identified. Several composite systems with various ply layup configurations are examined. Results are presented to illustrate the dependence of the residual stresses on the pertinent variables. The residual stresses are very sensitive to constituent material properties, composite stacking sequence and orientation, fiber content, and processing temperature. It is found that ply transverse tensile and in-plane shear residual stresses can reach magnitudes comparable to corresponding ply strengths and cause transply cracks in the composites. Residual stresses can also cause interply delamination. Ways to prevent transply cracking and interply delamination are recommended.

17. Key Words (Suggested by Author(s)) Fiber composites; Boron, S-Glass, graphite fibers; Metallic, nonmetallic; Residual stresses; Stress analysis; Structural analysis; Laminate theory; Transply cracking; Interply delamination		18. Distribution Statement Unclassified - unlimited	
19. Security Classif. (of this report) Unclassified	20. Security Classif. (of this page) Unclassified	21. No. of Pages 29	22. Price* $3.00

*For sale by the National Technical Information Service, Springfield, Virginia 22151

LAMINATION RESIDUAL STRESSES IN MULTILAYERED FIBER COMPOSITES

by Christos C. Chamis

Lewis Research Center

SUMMARY

Residual stresses arising from the lamination fabrication process of composites are investigated using linear laminate theory. The resulting equation for predicting residual stresses is presented. The variables that influence the residual stresses are identified. These variables are constituent materials and their thermal and elastic properties, average fiber diameter and number of fibers per end, fiber and void volume ratios; ply stacking sequence and orientation, and processing temperature. The effects of these variables on the residual stresses of several composite systems are examined. The fiber composites considered are boron/aluminum, boron/epoxy, S-glass/epoxy, Thornel-50 graphite/epoxy, and Modmor-I graphite/polyimide.

It was found that the residual transverse tensile and in-plane shear stresses can reach magnitudes comparable to the corresponding ply strengths and can cause transply cracking. The ply residual stresses are very sensitive to constituent material properties, ply stacking sequence and orientation, fiber content, and processing temperature. They are relatively insensitive to the void content. The residual stresses are relatively small in composites where the fiber content or the processing temperature vary only moderately from ply to ply. Ply residual stresses increase with increasing matrix modulus. They increase linearly with increasing matrix thermal coefficient of expansion. It is possible to orient plies in simulated components so that some plies have tensile longitudinal residual stress. Residual stresses can cause interply delamination due to the relative rotation of adjacent plies.

Residual stress transply cracking, in general, can be prevented by increasing the ply transverse tensile and shear strengths, decreasing the processing temperature, or decreasing the difference between the fiber and matrix thermal coefficients of expansion. In specific designs transply cracking can be prevented by suitable ply orientation, increase in fiber content, use of transitional plies, and reduction of the number of off-axis plies.

Experimental work to fully assess the residual stress effect on the structural response of the composite is suggested.

INTRODUCTION

Multilayered fiber composites are readily adaptable to simultaneous component and material designs. This approach allows the designer to take full advantage of the high stiffness and strength-to-density ratios of fiber composites. The result is an efficient use of fiber composite material in structural components. The composite is usually designed by specifying the fiber direction in each ply, the number of plies, and the fiber volume ratio necessary to meet the given loading requirements.

However, having different fiber directions in different plies can cause transply cracks such as have been observed in graphite-fiber composites. These cracks are caused by the large thermal residual stresses present in the composite. The residual stresses result from the fabrication process used to make fiber composites. The residual stresses arising from the fabrication process are examined quantitatively herein using linear laminate theory.

Multilayered fiber composites consist of several unidirectional layers (plies) oriented at specified angles relative to some coordinate axes system. The geometry of such a composite is depicted in figure 1. The plies consist of parallel fibers embedded in a matrix. The geometry of a ply is shown in figure 2. Glass or graphite fiber composites will have many filaments through the ply thickness.

In general, composites achieve their structural integrity as follows: Nonmetallic matrix composites are cured at elevated temperature under pressure; metallic matrix composites are either hot pressed or plasma sprayed. These methods induce residual stresses in the composite when it is at a temperature different from its cure or processing temperature. The difference between the cure or processing and the use temperature will be referred to here as temperature difference. The residual stresses can be either microresidual or macroresidual stresses.

The microresidual stresses are influenced by the local geometry of the constituents within the ply. They arise from the difference in the thermal coefficients of expansion of the constituents and the temperature difference. The matrix phase change shrinkage for resins also contributes to the microresidual stress. Adams, Doner, and Thomas (ref. 1) and Haener, Ashbaugh, Chia, and Feng (ref. 2), for example, treat this type of residual stress analytically. Marloff and Daniel (ref 3) and Koufopoulos and Theocaris (ref. 4) examined microresidual stress experimentally. The ply shown in figure 2 will have microresidual stresses.

Macroresidual stresses (ref. 5) are integrated averages through the ply thickness. These stresses have an effect on the ply similar to an equivalent thermal or mechanical load applied to the composite. They arise from the difference between the ply longitudinal and transverse thermal coefficients of expansion. Macroresidual stresses are present in those composites that have plies oriented at different angles and whose use

temperature differs from the cure or processing temperature. These stresses will be present in the composite depicted in figure 1.

The significance of the lamination residual stress was realized when transply cracks were observed in $0^{\circ}/90^{\circ}$ graphite composites. Doner and Novak (ref. 5) presented photomicrographs showing transply cracks. DeCrescente and Novak (ref. 6) and Winters (ref. 7) have observed similar cracks in other graphite/epoxy composites.

Some analytical treatment of the lamination residual stress has also been reported. Doner and Novak (ref. 5) considered the residual stresses in $0^{\circ}/90^{\circ}$ composites. Edighoffer, Ravenhall, and Juneau (ref. 8) examined the residual stresses in a boron/epoxy composite with laminations $\pm\theta/90$ where the $\pm\theta$ are considered as an equivalent 0° ply. This author (ref. 9) used linear laminate theory to predict residual stresses in graphite composites without restriction to ply orientation. The lamination theory used in reference 9 was developed in reference 10. It was implemented in references 11 to 13 and in a computer code (ref. 14).

The computer code of reference 14 provides a method for micromechanics, lamination, and stress analyses of multilayered fiber composites. The inputs to this code are constituent material properties, fiber and void contents, correlation coefficients, composite geometry, temperature difference (use temperature minus cure temperature), and composite stress resultants or displacements.

The computer code of reference 14 permits the variation of several basic parameters in fiber composites. It is used herein to investigate the residual stresses in laminated fiber composites. The following systems are examined: boron/aluminum, boron/epoxy, S-glass/epoxy, Thornel-50 graphite/epoxy, and Modmor-I graphite/polyimide. The significant parameters in these systems are ply orientation, fiber and void contents, matrix modulus of elasticity, matrix and thermal coefficients of expansion, and the temperature difference. To the author's knowledge, the effects of some of these parameters on the residual stresses are investigated for the first time. Also investigated for the first time are (1) possible ply delamination due to residual stress, and (2) residual stresses in composites which are unsymmetric with respect to bending.

The ply orientations examined are shown in table I together with the notation adopted herein for convenience. Theoretical thermal and elastic properties for the composite systems considered are listed in table II. These properties are for a fiber volume ratio of 0.55. The corresponding theoretical strength properties are given in table III. The results in tables II and III are those predicted by the computer code (ref. 14).

The significant parameters mentioned previously are varied in the computations. The results are plotted to illustrate the dependence of the ply residual stresses on these parameters as is described subsequently. The plots are grouped by composite system. The composite systems boron/aluminum, boron/epoxy, S-glass/epoxy, and Thornel-50 graphite/epoxy are used in some basic ply orientations. Results for various ply orien-

tations in composites unsymmetric with respect to bending are also presented for these systems. The composite system Modmor-I graphite/polyimide is used in simulated structural components. Some results are presented for this system to demonstrate possible ply delamination due to residual stresses.

The results presented herein are for three temperature differences: 900° F (773 K) for boron/aluminum, 300° F (440 K) for the boron/epoxy, S-glass/epoxy, and Thornel-50 graphite/epoxy systems, and 600° F (606 K) for the Modmor-I graphite/polyimide system. Residual stresses for any other temperature differences are obtained from the plots by direct proportion. This is possible because a linear theory is used and the residual stress is linearly dependent on the temperature difference.

Several recommendations are made for minimizing or eliminating the residual stress. These recommendations are deduced from the results presented and the equations used to predict the residual stresses. These equations are presented in their final form. The derivations are given in reference 10.

SYMBOLS

A_{cx}	array of composite extensional stiffnesses referred to composite structural axes
C_{cx}	array of composite coupling stiffnesses referred to composite structural axes
D_{cx}	array of composite bending stiffnesses referred to composite structural axes
E_{li}	array of strain-stress relations (elastic constants of the i^{th} ply)
E_{l11}	ply longitudinal modulus
E_{l22}	ply transverse modulus
G_{l12}	ply (in-plane) shear modulus
k_f, k_v	fiber and void volume ratios, respectively
$M_{c\Delta Tx}$	vector of unbalanced thermal moments referred to composite structural axes
$N_{c\Delta Tx}$	vector of unbalanced thermal forces referred to composite structural axes
R_{li}	array of transformation coefficients for the i^{th} ply
S_{l11T}	ply longitudinal tensile strength
S_{l11C}	ply longitudinal compressive strength
S_{l22T}	ply transverse tensile strength
S_{l22C}	ply transverse compressive strength

S_{l12S} ply in-plane shear strength

ΔT_{li} temperature difference for the i^{th} ply

x, y, z structural axes

z_{li} distance from reference plane to centroid of the i^{th} ply

1, 2, 3 material axes

α_{li} vector of thermal coefficients of expansion of the i^{th} ply referred to ply's material axes

α_{l11} ply longitudinal thermal coefficient of expansion

α_{l22} ply transverse thermal coefficient of expansion

β_{22T} correlation coefficient for ply transverse tensile strength

β_V void strain magnification coefficient

ϵ_{cox} vector of composite strains referred to composite structural axes at the reference plane

ϵ_{li} vector of strains for the i^{th} ply referred to ply's material axes

ϵ_{mpT} matrix allowable strain in tension

θ ply angle measured from the composite structural axes to the ply material axis 1

κ_{cx} composite local curvatures referred to composite structural axes

ν_{l12} ply Poisson's ratio in the two direction when the load is applied in the one direction

σ_{li} vector of ply stresses referred to ply's material axes

$\varphi_{\mu 22}$ strain magnification factor for ply transverse strength

{ } vector or column matrix

[ ] square array

GOVERNING EQUATIONS

The laminate theory equation for predicting the ply residual stresses is given by

$$\{\sigma_{li}\} = [E_{li}]^{-1}\langle [R_{li}]\{\epsilon_{cox}\} - z_{li}[R_{li}]\{\kappa_{cx}\} - \Delta T_{li}\{\alpha_{li}\}\rangle \tag{1}$$

The reference plane strains $\{\epsilon_{cox}\}$ and the curvature changes $\{\kappa_{cx}\}$ for a free com-

posite (no external loads and no boundary constraints) are computed from

$$\begin{Bmatrix} \{\epsilon_{cox}\} \\ \\ \{\kappa_{cx}\} \end{Bmatrix} = \begin{bmatrix} [A_{cx}][C_{cx}] \\ \\ [C_{cx}][D_{cx}] \end{bmatrix}^{-1} \begin{Bmatrix} \{N_{c\Delta Tx}\} \\ \\ \{M_{c\Delta Tx}\} \end{Bmatrix} \tag{2}$$

Equations (1) and (2) show that the ply residual stress is a function of the following factors: (1) the composite structural stiffness, (2) the ply spatial location in the composite, (3) the ply stress-strain relations, (4) the ply thermal coefficients of expansion, and (5) the temperature difference between the ply and the reference value. This difference equals the ply temperature minus the cure or processing temperature in computing residual stresses. The factors (1), (3), and (4) are related to the basic variables (constituent materials and thermoelastic properties, fiber and void volume ratios, number of plies, and ply orientation). These relations are given in either reference 10 or 14.

RESIDUAL STRESSES IN BORON/ALUMINUM COMPOSITES

The temperature difference selected for boron/aluminum composites is 900° F (773 K). The room temperature properties are used in the linear analysis. The applicability of linear analysis and room-temperature properties might be questioned for this temperature difference, particularly for the aluminum matrix. However, there are four reasons that justify this approach. First, the residual stresses are computed at room temperature. Second, the aluminum matrix modulus decreases with increasing temperature, but its thermal coefficient of expansion increases. These two effects tend to be compensatory. The third reason is that the results from a linear analysis can be scaled down proportionally to any desired temperature difference. The fourth reason is that composites that are designed to carry the residual stress at room temperature caused by a 900° F (773 K) temperature difference will be conservatively designed.

Ply residual transverse and shear stresses (as defined in fig. 2) are plotted as functions of ply orientation angle and fiber volume ratio in figure 3. The composite geometry and the temperature difference is noted in the captions of these figures.

Ply residual transverse stresses as a function of ply angle are plotted in figure 4 for the general composite geometry $8[0, 2(\pm\theta), 2(90), 2(\mp\theta), 0]$. The temperature difference and the fiber volume ratio (FVR) are 900° F (773 K) and 0.55, respectively. The results in this figure for $\theta = 0^{\circ}$ or 90° illustrate the dependence of the ply residual stress on the number of plies in each orientation.

Ply residual transverse stresses for composites of the following three geometries $8[4(+\theta), 4(-\theta)]$, $8(\pm\theta)$, $8[4(\pm\theta), 4(\mp\theta)]$ and with an FVR of 0.55 are plotted against θ in

figure 5. The ply considered in these composites is the first ply in the sequence. The composite geometry $8[4(+\theta), 4(-\theta)]$ represents a composite that is nonsymmetric with respect to bending. The composite geometry $8(\pm\theta)$ represents a composite that is nonsymmetric with respect to bending with interspersed plies. The composite geometry $8[4(\pm\theta), 4(\mp\theta)]$ represents a composite that is symmetric with respect to bending with interspersed plies.

The results in figures 3 to 5 show that the ply residual transverse and shear stresses increase with ply angle but decrease with fiber volume ratio. The smaller the number of plies in a given orientation, relative to other orientations in the same composite, the greater the residual stresses in these plies. The residual stresses in the outer plies of nonsymmetric noninterspersed composites are quite high. They are about twice as high as those in either nonsymmetric interspersed or symmetric interspersed plies. Introduction of $\pm 45^{\circ}$ plies for increased torsional stiffness produces high residual stresses. The residual stresses in quasi(pseudo)-isotropic symmetric composites (such as $8[0, 2(\pm 45), 2(90), 2(\mp 45), 0]$, fig. 6) are equal in all the plies.

The transverse ply tensile strength for a boron/aluminum unidirectional composite (ply) at an FVR of 0.55 is 14.1 ksi (97.1 MN/m^2) (see table III). This value is exceeded in many of the composites shown in figures 3 to 5.

To what extent the residual stresses can be annealed, if any, and how much these stresses affect the in-situ ply strength is not known. Also, the effect of creep in relieving residual stresses is not known at this time.

RESIDUAL STRESSES IN BORON, S-GLASS, AND THORNEL-50 GRAPHITE/EPOXY COMPOSITES

The residual stresses in these composites are computed from a 300° F (440 K) temperature difference, room temperature constituent material properties, and the linear theory available in reference 14. This theory is briefly described in the INTRODUCTION. Five reasons justify this approach: (1) The residual stresses are computed at room temperature. (2) Polymerization shrinkage (matrix phase change), though not accounted for directly in the theory, is compensated for by the higher temperature. (3) The epoxy modulus decreases with increasing temperature, but the epoxy thermal coefficient of expansion increases. (4) The residual stress results presented, herein, can be scaled down proportionally to any desired temperature difference. (5) Composites designed to withstand the residual stress at room temperature predicted by this approach will be conservatively designed.

Results for ply residual transverse stresses are presented. These stresses are primarily responsible for the transply cracking.

Boron/Epoxy Composites

The residual transverse stresses in the $\pm\theta$ plies of the boron/epoxy composites $8[2(0), 2(\pm\theta), 2(\mp\theta), 2(0)]$ are plotted against θ and three fiber volume ratios in figure 6(a).

Ply residual transverse stresses for the 0°, $\pm\theta^{\circ}$, and 90° plies of the composites $8[0, 2(\pm\theta), 2(90), 2(\mp\theta), 0]$ are plotted against θ in figure 6(b). The FVR is 0.55 for these composites. The results in this figure at $\theta = 0^{\circ}$ and 90° illustrate the effect on residual stress of the numbers of plies in each orientation.

The residual transverse stress in the outer ply of the composites $8[4(+\theta), 4(-\theta)]$, $8(\pm\theta)$, and $8[4(\pm\theta), 4(\mp\theta)]$ is plotted against θ in figure 6(c). The FVR is 0.55 for these composites. The composites $8[4(+\theta), 4(-\theta)]$ are nonsymmetric with respect to bending and have a noninterspersed ply stacking sequence. The composites $8(\pm\theta)$ are nonsymmetric with respect to bending but do have an interspersed ply stacking sequence. The composites $8[4(\pm\theta), 4(\mp\theta)]$ are symmetric and have interspersed ply sequence.

The transverse strength for the unidirectional composite (ply) at an FVR of 0.55 is 8.6 ksi (59.3 MN/m^2) (see table III). This value is exceeded only by the residual stresses in the outer plies of the composite $8[4(+\theta), 4(-\theta)]$ (fig. 6(c)). However, the margin of safety is about 0.3 in many of the other composites.

Several interesting points are illustrated by the results shown in figure 6: (1) The ply residual transverse stress in boron/epoxy composites is relatively high when compared with the ply transverse strength for some composite geometries. (2) The ply residual stress is quite sensitive to the ply angle, but not as sensitive to FVR. (3) The ply transverse residual stresses in the composites $8[0, 2(\pm\theta), 2(90), 2(\mp\theta), 0]$ are practically invariant with θ. (4) Nonsymmetric noninterspersed-ply composites experience high ply residual stresses when compared with other composite geometries. (5) Nonsymmetric interspersed-ply and symmetric interspersed-ply composites experience ply residual stresses of about the same magnitude.

S-Glass/Epoxy Composites

The residual transverse stress in the $\pm\theta$ ply of the S-glass/epoxy composites $8[2(0), 2(\pm\theta), 2(\mp\theta), 2(\theta)]$ is plotted against θ and three FVR in figure 7(a).

Ply residual transverse stresses for the 0°, $\pm\theta^{\circ}$, and 90° plies of the composites $8[0, 2(\pm\theta), 2(90), 2(\mp\theta), 0]$ are plotted against θ in figure 7(b). The FVR is 0.55 for these composites. The results in this figure for $\theta = 0^{\circ}$ and 90° illustrate the effect on residual stress of the number of plies in each orientation.

The residual transverse stresses in the outer ply of the composites $8[4(+\theta), 4(-\theta)]$, $8(\pm\theta)$, and $8[4(\pm\theta), 4(\mp\theta)]$ are plotted against θ in figure 7(c). The FVR is 0.55 for

these composites. The composites $8[4(+\theta), 4(-\theta)]$ are nonsymmetric noninterspersed-ply composites. The composites $8(\pm\theta)$ are nonsymmetric interspersed-ply composites. The composites $8[4(\pm\theta), 4(\mp\theta)]$ are symmetric interspersed-ply composites.

The transverse strength for the S-glass/epoxy unidirectional composite (ply) at an FVR of 0.55 is 4.4 ksi (30.4 MN/m^2) (see table III). This value is very close to the ply residual stress of several composites. It is exceeded in the outer plies of some composites $8[4(+\theta), 4(-\theta)]$. This implies that S-glass/epoxy composites of the geometries and FVR examined in figure 7 could experience transply cracks. This will not be the case if the transverse strength of the plies is much greater than 4.4 ksi (see, e.g., table I of ref. 5).

Several interesting points are illustrated by the results in figure 7. (1) The calculated ply residual transverse stress could exceed the ply transverse strength. The extent that the ply transverse strength is exceeded by the calculated ply residual stress depends on composite geometry. (2) The ply residual stress is quite sensitive to ply orientation angle in certain composite geometries. (3) The ply residual stress is relatively insensitive to fiber volume ratio in composites with less than 0.55 FVR. (4) The ply residual stress is sensitive to the number of plies in each orientation. (5) Nonsymmetric noninterspersed-ply composites experience comparatively large ply residual stresses. (6) Nonsymmetric interspersed-ply and symmetric interspersed-ply composites experience ply residual stresses of about the same magnitude.

Thornel-50 Graphite/Epoxy Composites

The residual transverse stress in the $\pm\theta$ ply of the Thornel-50 graphite/epoxy composites $8[2(0), 2(\pm\theta), 2(\mp\theta), 2(0)]$ is plotted against θ and three values of FVR in figure 8(a).

Ply residual transverse stresses for the 0°, $\pm\theta^\circ$, and 90°-plies of the composites $8[0, 2(\pm\theta), 2(90), 2(\mp\theta), 0]$ are plotted against θ in figure 8(b). The FVR is 0.55 for these composites. The results in this figure for $\theta = 0^\circ$ and 90° illustrate the effect on residual stress of the number of plies in each orientation.

The residual transverse stress in the outer ply of the composites $8[4(+\theta), 4[-\theta)]$, $8(\pm\theta)$, and $8[4(\pm\theta), 4(\mp\theta)]$ is plotted against θ in figure 8(c). The FVR is 0.55 for these composites. The composites $8[4(+\theta), 4(-\theta)]$ are nonsymmetric noninterspersed-ply composites. The composites $8(\pm\theta)$ are nonsymmetric interspersed-ply composites. The composites $8[4(\pm\theta), 4(\mp\theta)]$ are symmetric interspersed-ply composites.

The transverse strength for the Thornel-50 graphite/epoxy unidirectional composite (ply) at an FVR of 0.55 is 3.7 ksi (25.5 MN/m^2) (see table III). This value is exceeded, or nearly so, by several composites. This implies that plies in Thornel-50 graphite/

epoxy composites of the geometries and values of FVR examined in figures 8(a) to 8(c) will experience transply cracks. This has been observed experimentally (refs. 5 to 7). This will not be the case if the transverse strength of the plies is about 8.0 ksi (55.2 MN/m^2).

Several interesting points are illustrated by the results in figure 8. (1) The calculated ply residual transverse stress exceeds the ply transverse strength. The extent that the ply transverse strength is exceeded by the calculated ply residual stress depends on composite geometry. (2) The ply residual stress is quite sensitive to ply angle in certain composite geometries. (3) The ply residual stress is sensitive to FVR. (4) The ply residual stress is insensitive to the number of plies in each orientation. It is relatively insensitive to θ in the composites $8[0, 2(\pm\theta), 2(90), 2(\mp\theta), 0]$. (5) Nonsymmetric noninterspersed-ply composites experience ply residual stress that is about 30 percent higher than other composite geometries. (6) Nonsymmetric interspersed-ply and symmetric interspersed-ply composites experience ply residual stresses of about the same magnitude.

SIMULATED COMPOSITE COMPONENTS

The residual stresses in the plies of two simulated composite components were studied. The composite geometries are $24[4(\pm 30), 2(\pm 15), 12(0), 2(\mp 15), 4(\mp 30)]$ and $24[4(\pm 45), 2(\pm 22.5), 12(0), 2(\mp 22.5), 4(\mp 45)]$. The composite system is Modmor-I graphite/polyimide, and it is used for elevated temperature application. The temperature difference for this system is about 600° F (606 K).

The dependence of the ply residual stresses on several factors is examined. These factors are (1) fiber volume ratio (FVR), (2) void content, (3) variation of the FVR from ply to ply within the same composite, (4) different groups of plies with different FVR, (5) variations in the matrix thermal coefficient of expansion, and (6) variations in the matrix modulus. Also, the effect of the residual stresses on the relative rotation of adjacent plies is investigated.

The computations are based on a 600° F (606 K) temperature difference and room-temperature constituent material properties. The justification for this approach is the same as that given for the other fiber/epoxy composite systems. (See section Residual Stresses in Boron, S-Glass, and Thornel-50/Epoxy Composites.)

The ply residual transverse stress is plotted against FVR in figure 9(a) for both components. Results for the ply residual longitudinal stress are shown in figure 9(b). The residual longitudinal stress in the 0° plies of both components is tensile. Results for ply residual shear stress are plotted against FVR in figure 9(c). The results in these figures show that the ply residual stresses are sensitive to both composite geometry and FVR.

The void content effect on the ply transverse residual stress is illustrated in figure 10. This effect is negligible for all practical purposes. However, it is important to keep in mind that the ply transverse strength decreases with increasing void content (ref. 12). The decrease in ply transverse strength could produce transply cracks at smaller temperature differences. Proper consideration of the void effects is necessary to avoid transply cracking. (See eq. (3) in this section.)

The effects of variable ply FVR on the ply transverse residual stresses are shown in figure 11 for one component only. These effects are negligible as can be seen in the figure. Having different groups of plies at different FVR has a negligible effect on the ply residual transverse stress. This is illustrated in figure 12. Negligible effects were found also when the ply temperature was varied similar to the FVR. These results are not presented here.

The dependence of the ply residual transverse stress on the matrix thermal coefficient of expansion is illustrated in figure 13. Two important points are observed here: (1) The ply residual stress varies linearly with matrix thermal coefficient of expansion and (2) the residual stresses can be reduced by decreasing the magnitude of the thermal coefficient of the matrix. The effects of varying the fiber thermal coefficients of expansion will produce an effect opposite to those shown in figure 13 for the thermal coefficient of the matrix. This implies that increasing the fiber thermal coefficient of expansion is another effective way to reduce the residual stress.

The dependence of the ply residual transverse stress on the matrix modulus is illustrated in figure 14. The results in this figure show that the residual stress increases nonlinearly with increasing matrix modulus. This increase is quite rapid at modulus values of 100 to 700 ksi (690 MN/m^2) and not as rapid at modulus values greater than 700 ksi (4.8 MN/m^2).

The results in figure 14 should be examined jointly with the ply transverse strength before any meaningful conclusions are made. The ply transverse strength is given by the expression (ref. 12).

$$S_{l22T} = \beta_{22T} \frac{\epsilon_{mpT}}{\beta_v \varphi_{\mu 22}} E_{l22} \qquad (3)$$

where S_{l22T} is the ply transverse tensile strength, β_{22T} is the correlation factor, ϵ_{mpT} is the allowable matrix tensile strain to denote failure, β_v is the void strain magnification factor, $\varphi_{\mu 22}$ is the strain magnification factor, and E_{l22} is the ply transverse modulus. The variables ϵ_{mpT}, $\varphi_{\mu 22}$, and E_{l22} are not independent of the matrix modulus. For example, $\varphi_{\mu 22}$ decreases but E_{l22} increases with increasing matrix modulus (ref 10), and ϵ_{mpT} increases with increasing matrix modulus in general.

The following point can be made in view of the preceding discussion. The ply transverse residual stresses increase with increasing matrix modulus. The ply transverse strength also increases with increasing matrix modulus. Transply cracking will eventually occur if the ply residual transverse stress increases at a higher rate than the ply transverse strength. Limited results showed that the ply transverse strength increases at a higher rate than the residual stress for some graphite composites during this investigation.

The effect of the residual stress on the adjacent ply relative rotation is illustrated in figure 15. Relative rotation is plotted against fiber volume ratio for selected adjacent plies of the two components. The estimated allowable relative rotation is also plotted in the figure, and the prediction of it is discussed in references 10 and 11. The results in figure 15 show that residual stresses could cause interply delaminations. The delamination depends on the constituent materials and composite geometry, the ply angles of the two adjacent plies, and the fiber and void volume ratios. It is interesting to note that the component with the $\pm 30^{\circ}$ and $\pm 15^{\circ}$ plies has a higher probability of interply delamination than the component with the $\pm 45^{\circ}$ and $\pm 22.5^{\circ}$ plies. The component with the $\pm 30^{\circ}$ and $\pm 15^{\circ}$ plies is superior in all other respects with respect to residual stress. To the author's knowledge, the significance of the results in figure 25 has not been recognized by other investigators to date.

The results in figures 16 to 25 show that composites designed by neglecting the residual stresses will be unconservative in some loading conditions.

The effects of introducing transitional plies (intermediate plies for less-abrupt orientation transition between groups of plies) or decreasing the number of off-axis plies on the residual stress are illustrated in figure 16. The residual transverse stress in the $\pm 45^{\circ}$ plies is plotted against FVR. The composite with the transitional plies is denoted by the long-dashed curve. The composite in which the transitional plies have been incorporated with the face (surface) plies is denoted by the solid curve. The composite in which the transitional plies have been incorporated in the core plies is identified by the short-dashed curve.

The results in figure 16 show that both reduction of the number of off-axis plies and introduction of transitional plies reduce the residual stress by small amounts. The number of off-axis plies is controlled by strength and stiffness requirements and changes might not be permitted in specific designs.

WAYS TO MINIMIZE OR ELIMINATE LAMINATION RESIDUAL STRESSES

Several alternatives are possible for minimizing or eliminating the lamination residual stresses. These alternatives may be grouped into two categories. The first

category is general, and the second is for specific designs. They are summarized briefly.

In general, residual stresses at room temperature can be reduced or eliminated by

(1) Use of lower cure or processing temperature matrices

(2) Decreasing the difference between the fiber and the matrix thermal coefficients of expansion

(3) Increasing the allowable elongation of the matrix at failure with a simultaneous increase in the matrix modulus.

In specific designs, the residual stress can be reduced by

(1) Proper selection of composite system

(2) Suitable ply orientation and stacking sequence

(3) Appropriate selection of the number of plies in each direction

(4) Introduction of transitional plies

(5) Decreasing the number of off-axis plies if stiffness and strength requirements permit it

(6) Increasing the fiber volume ratio

(7) Any possible combination of these.

EXPERIMENTAL WORK NEEDED

Both theory and experiment show that the ply residual transverse stresses due to lamination are of magnitudes comparable to those of the ply transverse strengths. However, four important questions need to be answered before the effect of residual stresses on the composite structural response can be realistically assessed: (1) decay of residual stress with time, (2) effect of transply cracks on composite stiffness, (3) effect of transply cracks on composite strengths, and (4) effect of transply cracks on composite degradation by the environment.

These questions can be answered best by simple but strategic experimental investigation. Bending tests in fatigue and creep should provide qualitative answers to these questions.

CONCLUSIONS

The results of this theoretical investigation, which is based on linear laminate theory and on a semiempirical micromechanics theory, lead to the following conclusions.

1. The ply residual transverse stress is generally tensile. The residual stress

depends on the composite system, ply orientation, fiber volume ratio, and processing conditions. The residual stress can be large relative to transverse strength for graphite/epoxy and boron/aluminum composites.

2. The ply residual in-plane shear stress can be comparable to the ply's shear strength.

3. The ply residual transverse or shear stress can be comparable to the corresponding ply strengths in simulated components. This can cause transply cracking. It can also reduce the ply capacity to carry transverse tensile or in-plane shear loads.

4. The ply residual stresses are very sensitive to temperature difference, ply orientation, number of plies in each direction and to fiber volume ratio.

5. The ply residual stresses are relatively insensitive to void content and to moderate ply-to-ply fiber volume ratio and processing temperature variations.

6. The ply residual stresses generally increase with increasing ply orientation angle.

7. The ply residual stresses increase nonlinearly with increasing matrix modulus. They increase linearly with the matrix coefficients of expansion.

8. It is possible to orient plies in simulated components so that some plies have tensile longitudinal residual stress. However, the residual longitudinal stress is usually compressive. Its magnitude is usually 15 to 20 percent of the ply's corresponding compressive strength.

9. Transply residual stress cracking, in general, can be prevented by increasing the ply transverse and shear strengths, and decreasing the processing temperature. It can be prevented by decreasing the difference between the thermal coefficients of the fiber and the matrix sufficiently.

10. In specific designs, cracking can be prevented by suitable ply orientation, variation of the number of plies in each direction, introduction of transitional plies, reduction of the number of off-axis plies, increasing the fiber content (within practical limits), or by any combination of these.

11. Neglecting the residual stresses in designing with fiber composites can lead to unconservative design.

12. Experimental work is needed for a realistic assessment of residual stresses on composite structural response.

Lewis Research Center,
National Aeronautics and Space Administration,
Cleveland, Ohio, October 5, 1970,
129-03.

REFERENCES

1. Adams, D. F.; Doner, D. R.; and Thomas, R. L.: Mechanical Behavior of Fiber-Reinforced Composite Materials. Report No. AFML - TR-67-96, Aeronutronic, May, 1967.

2. Haener, J.; Ashbaugh, N.; Chia, Y-C.; and Feng, N-Y.: Investigation of Micromechanical Behavior of Fiber Reinforced Plastics. Rept. No. USAAVLABS - TR-67-66, Whittaker Corp. Warnco Res. and Development Div., Feb. 1968.

3. Marloff, R. H.; and Daniel, I. M.: Three-Dimensional Photoelastic Analysis of a Fiber-Reinforced Composite Model. Experimental Mechanics, Vol. 9, No. 4, Apr. 1969, pp. 156-162.

4. Koufopoulos, T.; and Theocaris, P. S.: Shrinkage Stresses in Two-Phase Materials, J. Composite Materials. Vol. 3, Apr. 1969, pp. 308-320.

5. Doner, D. R.; and Novak, R. C.: Structural Behavior of Laminated Graphite Filament Composites. Proceedings of the 24th Annual Society of the Plastics Industry Conference, 1969, pp. 1-D - 2-D.

6. DeCrescente, M. A.; and Novak, R. C.: Fabrication Stresses in Graphite-Resin Composites, Paper No. 70-GT-84, ASME, May, 1970.

7. Winters, W. E.: Thermal Anisotropic Behavior in Graphite-Epoxy Composites, Paper No. 70-GT-129, ASME, May, 1970.

8. Edighoffer, H.; Ravenhall, R.; and Juneau, Jr., P. W.: Analysis and Structural Verification of Boron Filament Wound Composites, Proceedings of the 25th Annual Society of the Plastics Industry Conference, 1970, pp. 1-D - 12-D.

9. Chamis, C. C.: Design and Analysis of Fiber Composite Structural Components. Proceedings of the Aerospace Structural Materials Conference, NASA SP-227, 1970, pp. 217-228.

10. Chamis, C. C.: Design Oriented Analysis and Structural Synthesis of Multilayered-Filamentary Composites. Ph.D. Thesis, Case-Western Reserve University, 1967.

11. Chamis, C. C.: Important Factors in Fiber Composite Design. Proceedings of the 24th Annual Society of the Plastics Industry Conference, 1969, pp. 1-E - 18-E.

12. Chamis, C. C.: Failure Criteria for Filamentary Composites. NASA TN D-5367, 1969.

13. Chamis, C. C.: Characterization and Design Mechanics for Fiber-Reinforced Metals. NASA TN D-5784, 1970.

14. Chamis, C. C.: Computer Code for the Analysis of Multilayered Fiber Composites - Users Manual. NASA TN D-7013, 1970.

TABLE I. - COMPOSITE GEOMETRY AND NOTATION IDENTIFICATION

Composite	Ply number								Notation
	1	2	3	4	5	6	7	8	
	Ply orientation angle, deg								
1	0^o	0^o	$+\theta$	$-\theta$	$-\theta$	$+\theta$	0^o	0^o	$8[2(0), 2(\pm\theta), 2(\mp\theta), 2(0)]$
2	0^o	$+\theta$	$-\theta$	90^o	90^o	$-\theta$	$+\theta$	0^o	$8[0, 2, (\pm\theta)2(90), 2(\mp\theta), \theta]$
3	$+\theta$	$-\theta$	$+\theta$	$-\theta$	$-\theta$	$+\theta$	$-\theta$	$+\theta$	$8[4(\pm\theta), 4(\mp\theta)]$
4	$+\theta$	$-\theta$	$+\theta$	$-\theta$	$+\theta$	$-\theta$	$+\theta$	$-\theta$	$8(\pm\theta)$
5	$+\theta$	$+\theta$	$+\theta$	$+\theta$	$-\theta$	$-\theta$	$-\theta$	$-\theta$	$8[4(+\theta), 4(-\theta)]$

TABLE II. - THEORETICAL UNIAXIAL PLY ELASTIC AND THERMAL PROPERTIES

OF VARIOUS COMPOSITES AT ROOM TEMPERATURE

[Normalized at 0.55 fiber volume ratio and zero voids (refs. 12 and 13).]

Composite system	Elastic modulus						Poisson's ratio	Thermal coefficient of expansion			
	Longitudinal		Transverse		Shear			Longitudinal		Transverse	
	psi	GN/m^2	psi	GN/m^2	psi	GN/m^2		in./in./$^{\circ}$F	cm/cm/K	in./in./$^{\circ}$F	cm/cm/K
Boron/aluminum	37.5×10^6	258.6	26.9×10^6	185.5	13.2×10^6	91.0	0.23	4.0×10^{-6}	7.2×10^{-6}	6.2×10^{-6}	11.2×10^{-6}
Boron/epoxy	33.2×10^6	228.9	2.1×10^6	14.5	1.0×10^6	6.9	.24	3.0×10^{-6}	5.4×10^{-6}	14.2×10^{-6}	25.6×10^{-6}
S-glass/epoxy	7.0×10^6	48.3	1.7×10^6	11.7	$.9\times10^6$	6.2	.25	3.7×10^{-6}	6.7×10^{-6}	14.1×10^{-6}	25.4×10^{-6}
Thornel-50 graphite/epoxy	27.8×10^6	191.7	1.0×10^6	6.9	$.7\times10^6$	4.8	.24	$-.1\times10^{-6}$	$-.18\times10^{-6}$	20.6×10^{-6}	37.1×10^{-6}
Modmor-I graphite/polyimide	33.2×10^6	228.9	$.9\times10^6$	6.2	$.6\times10^6$	4.1	.24	$-.3\times10^{-6}$	$-.54\times10^{-6}$	20.5×10^{-6}	36.9×10^{-6}

TABLE III. - THEORETICAL UNIAXIAL STRENGTHS OF VARIOUS COMPOSITES AT ROOM TEMPERATURE

[Normalized at 0.55 fiber volume ratio and zero voids (refs. 12 and 13).]

Composite system	Uniaxial strength at room temperature									
	S_{l11T}		S_{l11C}		S_{l22T}		S_{l22C}		S_{l12S}	
	ksi	MN/m^2	ksi	MN/m^2	ksi	MN/m^2	ksi	MN/m^2	ksi	MN/m^2
Boron/aluminum	176	1214	185	1276	14.7	101	16.1	111	15.9	110
Boron/epoxy	214	1476	188	1296	8.6	59.3	30.1	208	13.6	93.8
S-glass/epoxy	204	1407	143	986	4.4	30.3	28.3	195	8.3	57.2
Thornel-50 graphite/epoxy	106	731	56.6	390	3.7	25.5	17.6	121	2.6	17.9
Modmor-I graphite/polyimide	138	952	136	938	6.1	42.1	19.7	136	7.8	53.8

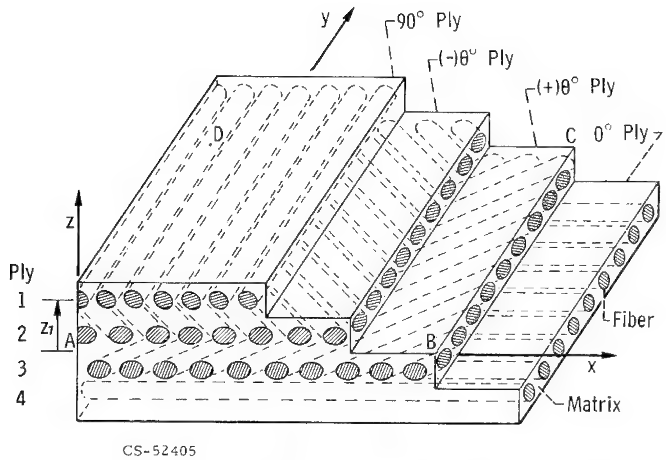

Figure 1. - Typical fiber composite geometry (plane ABCD is the reference plane).

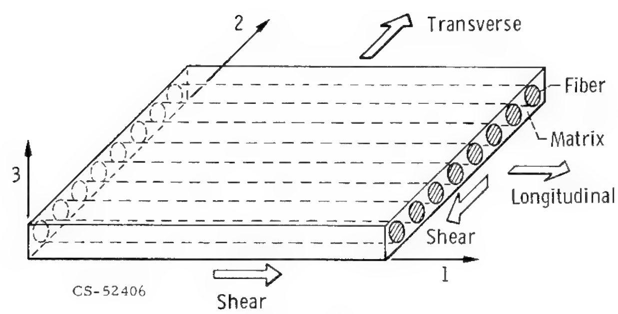

Figure 2. - Single ply.

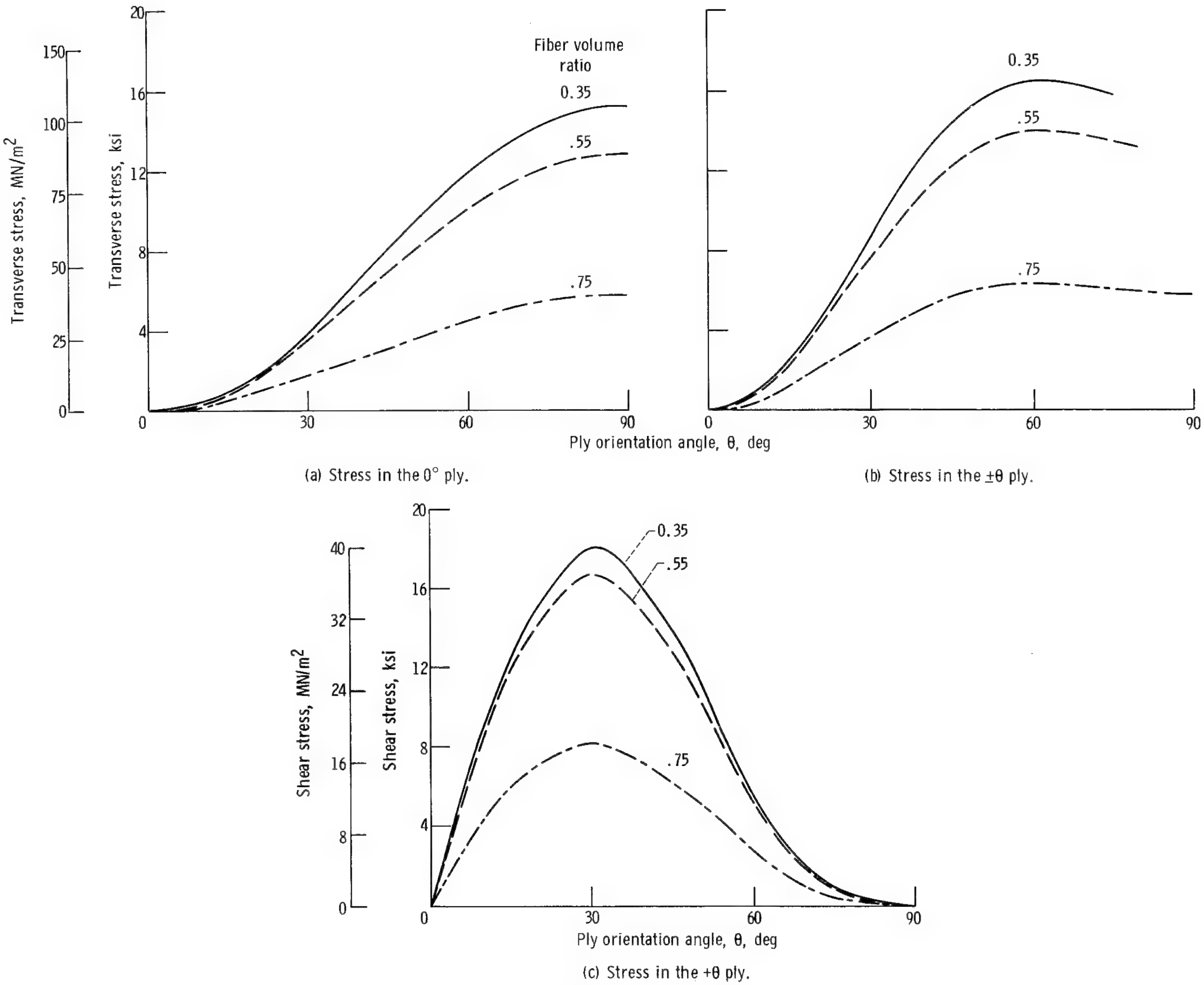

Figure 3. - Ply residual stress for boron/aluminum composite. Composite geometry, 8[2(0), 2(±θ), 2(∓θ), 2(0)]; temperature difference, 900° F (773 K).

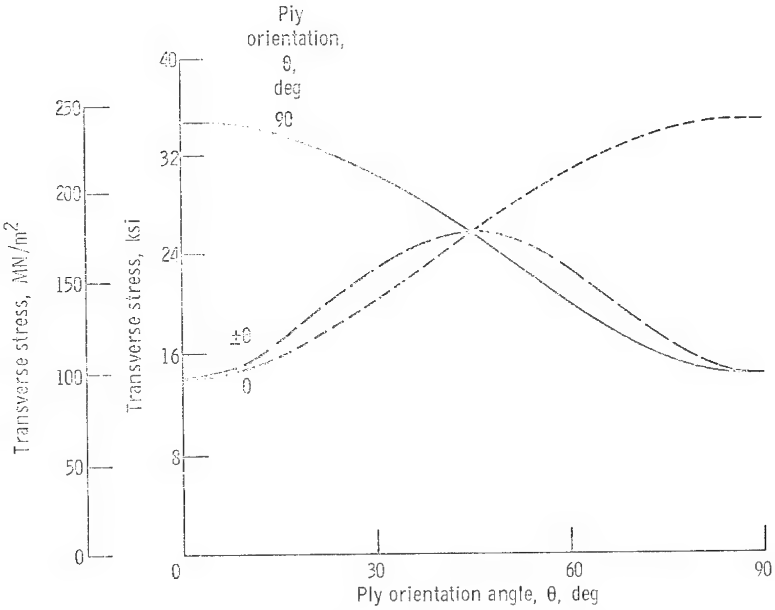

Figure 4. - Ply residual transverse stress for boron aluminum composites. Composite geometry, $8[0,\ 2(\pm\theta),\ 2(90),\ 2(\mp\theta),\ 0]$; fiber volume ratio, 0.55; temperature difference, 900° F (773 K).

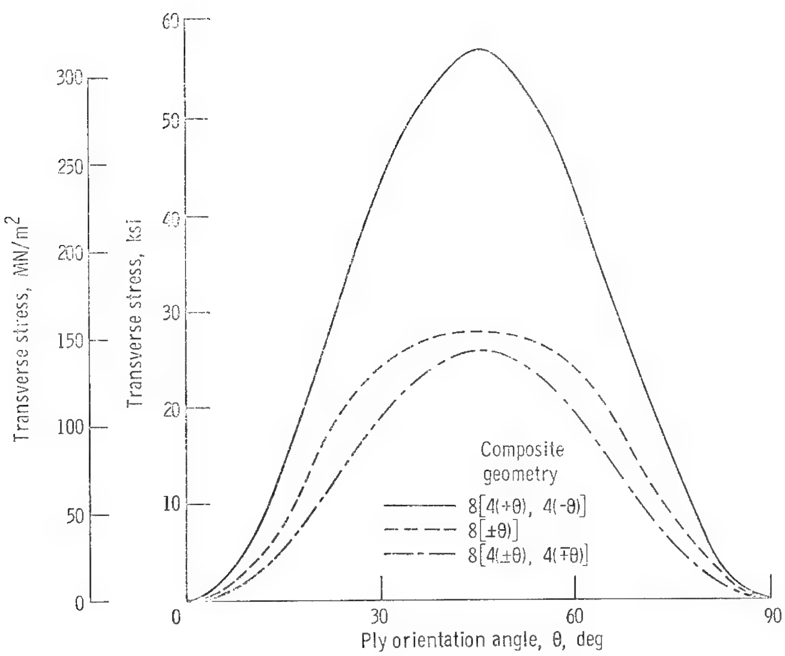

Figure 5. - Outer-ply residual transverse stress for boron aluminum composites. Fiber volume ratio, 0.55; temperature difference, 900° F (773 K).

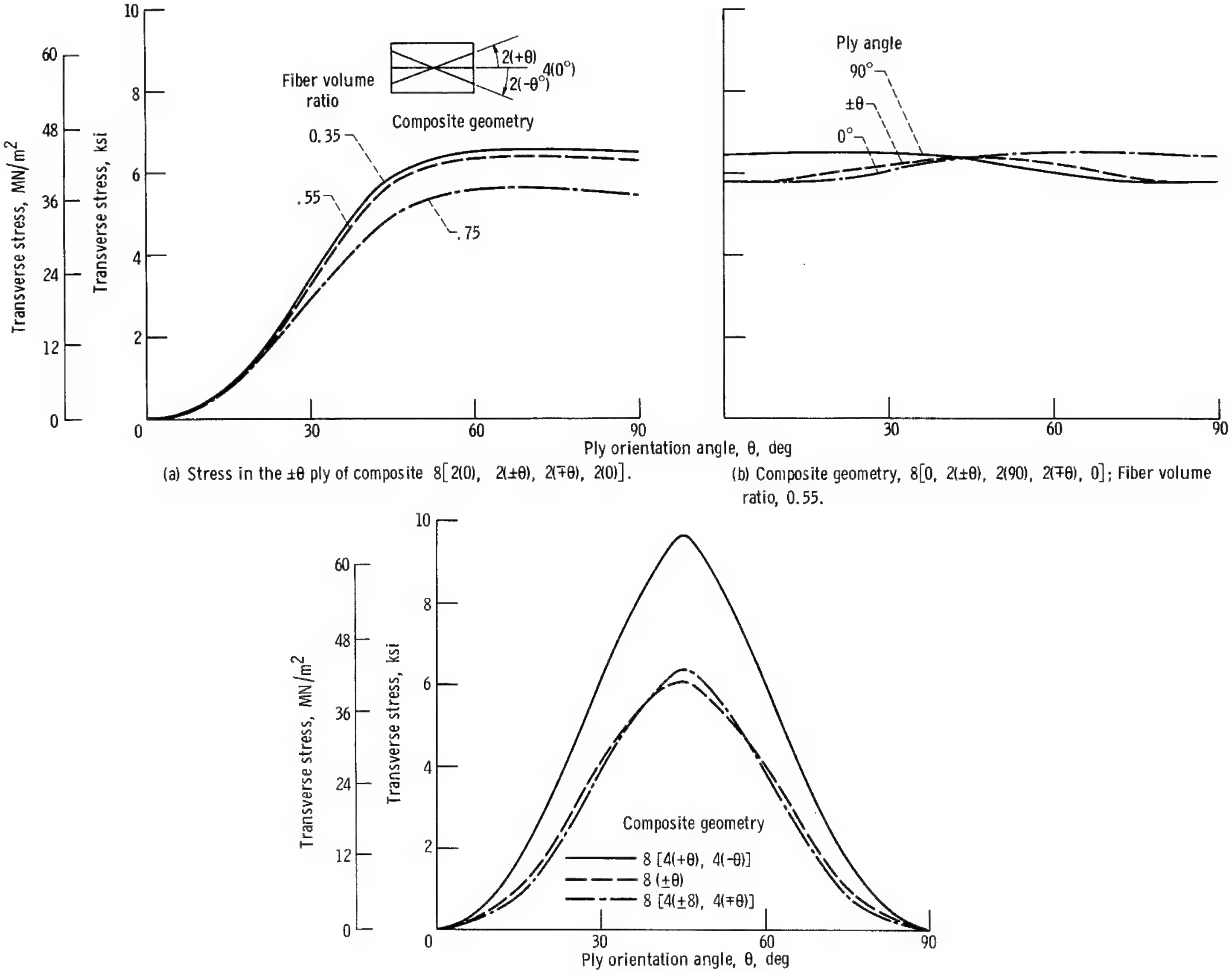

(a) Stress in the ±θ ply of composite 8[2(0), 2(±θ), 2(∓θ), 2(0)].

(b) Composite geometry, 8[0, 2(±θ), 2(90), 2(∓θ), 0]; Fiber volume ratio, 0.55.

(c) Outer ply; fiber volume ratio, 0.55.

Figure 6. - Ply transverse residual stress for boron/epoxy composites. Temperature difference, 300° F (440 K).

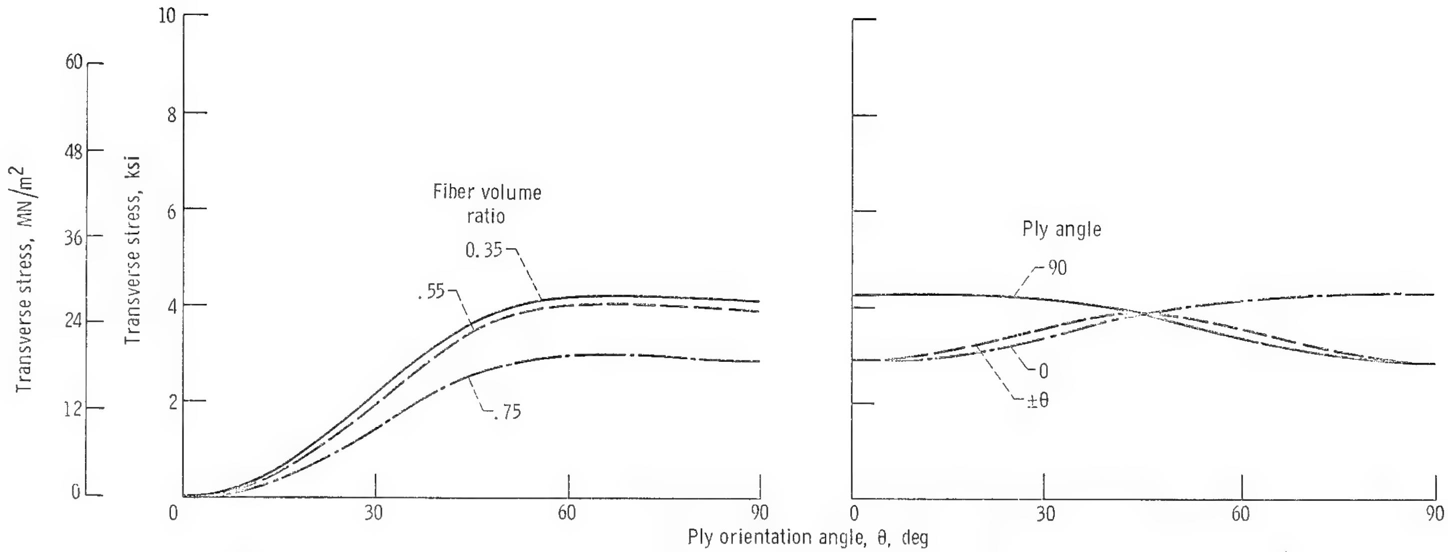

(a) Stress in the +θ ply of composite 8[2(0), 2(±θ), 2(∓θ), 2(0)].

(b) Composite geometry 8[0, 2(±θ), 2(90), 2(∓θ), 0].

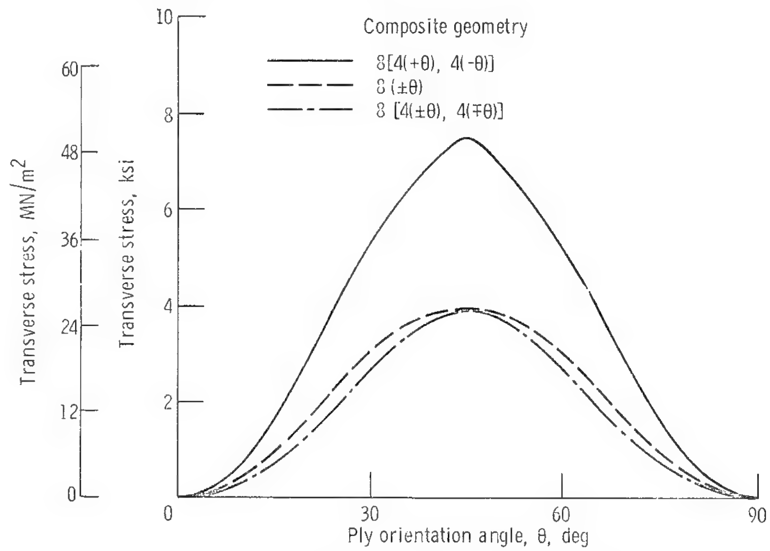

(c) Outer ply; fiber volume ratio, 0.55.

Figure 7. - Ply residual transverse stress for S-glass/epoxy composites. Temperature difference, 300° F (440 K).

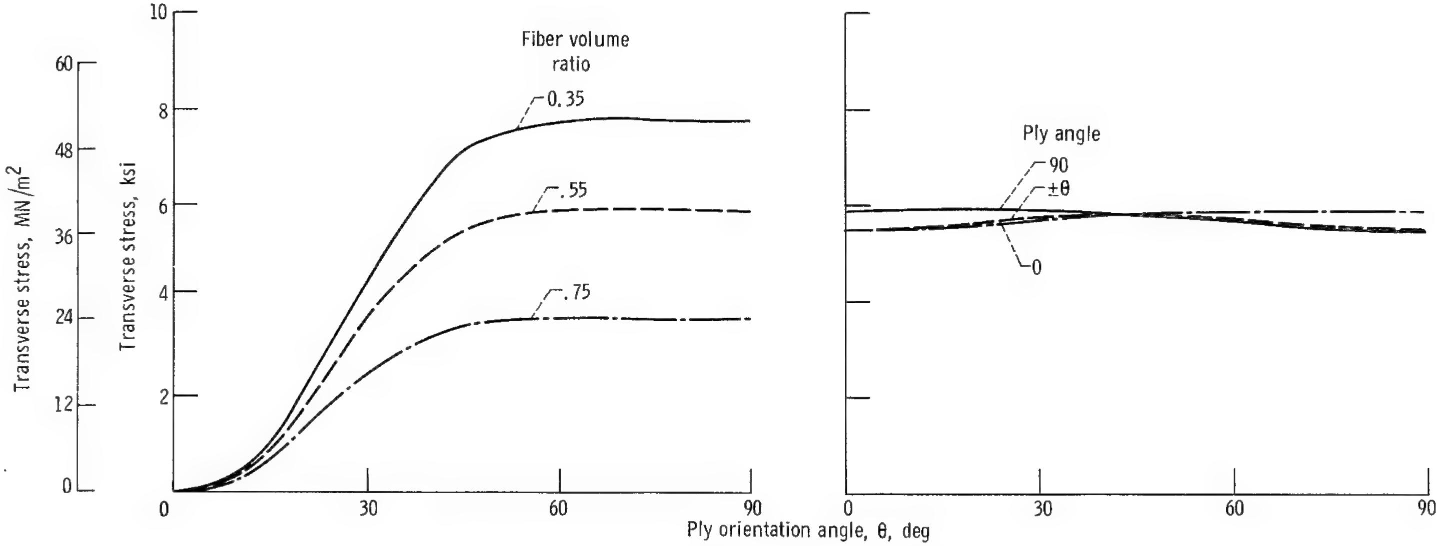

(a) Stress in the +θ ply of composite 8[2(0), 2(±θ), 2(∓θ), 2(0)].

(b) Composite geometry, 8[0, 2(±θ), 2(90), 2(∓θ), 0]; fiber volume ratio, 0.55.

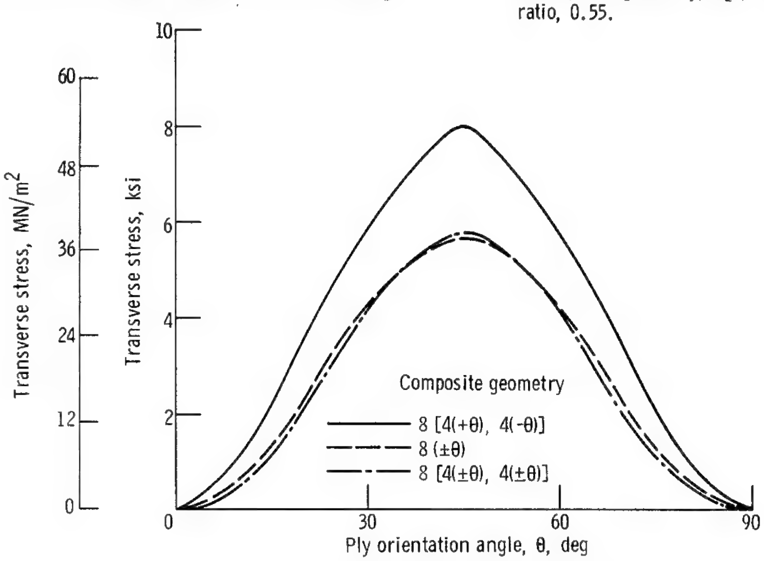

(c) Outer ply; fiber volume ratio, 0.55.

Figure 8. - Ply residual transverse stress for graphite Thornel-50/epoxy composites. Temperature difference, 300° F (440 K).

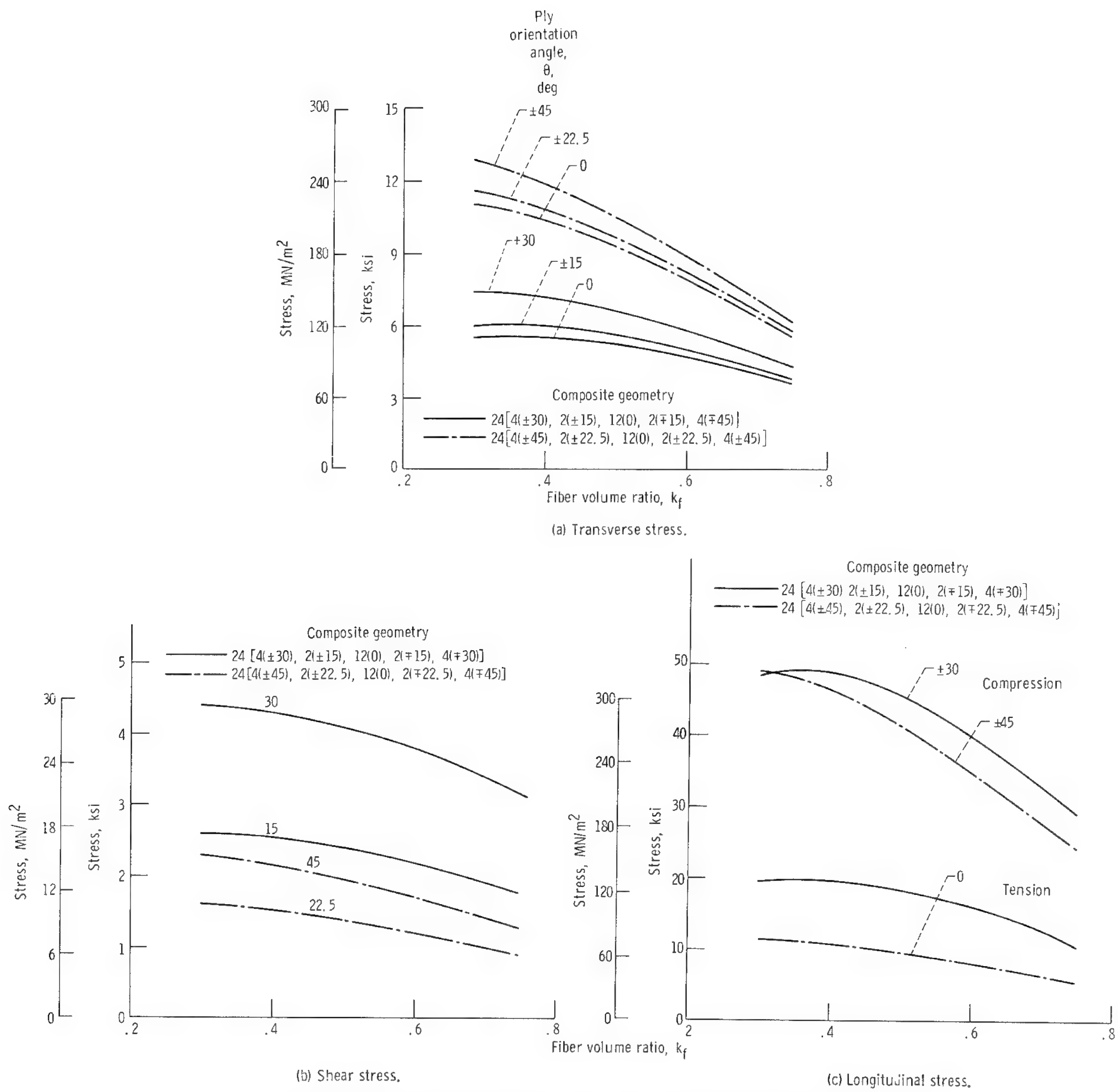

Figure 9. - Ply residual stress for Modmor-I/polyimide composites. Temperature difference, 600° F (606 K).

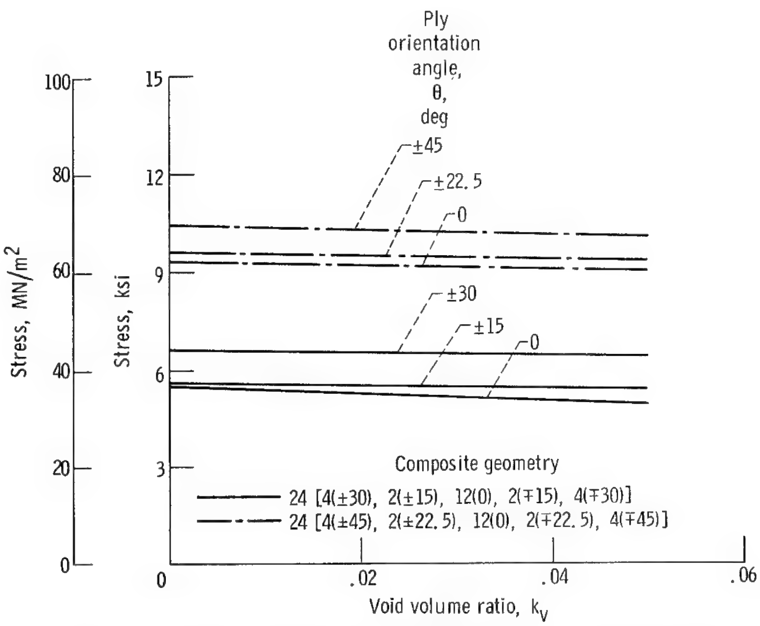

Figure 10. - Effects of voids on ply transverse residual stress. Modmor-I/polyimide composites; fiber volume ratio, 0.50; temperature difference, 600° F (606 K).

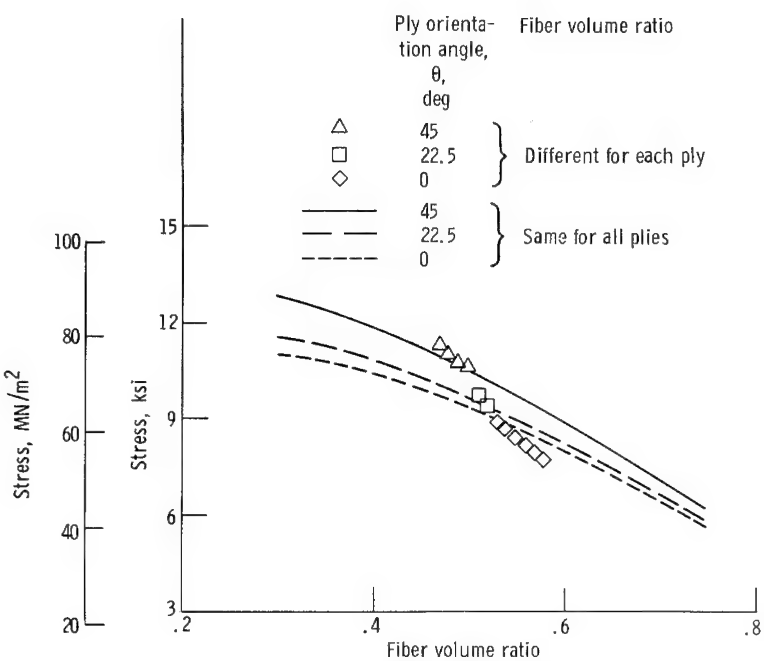

Figure 11. - Effects of variable fiber volume ratio on ply residual stress. Modmor-I/polyimide composite; composite geometry, 24[4 (±45), 2(±22.5), 12(0), 2(∓22.5), 4(∓45)]; void volume ratio, 0; temperature difference, 600° F (606 K).

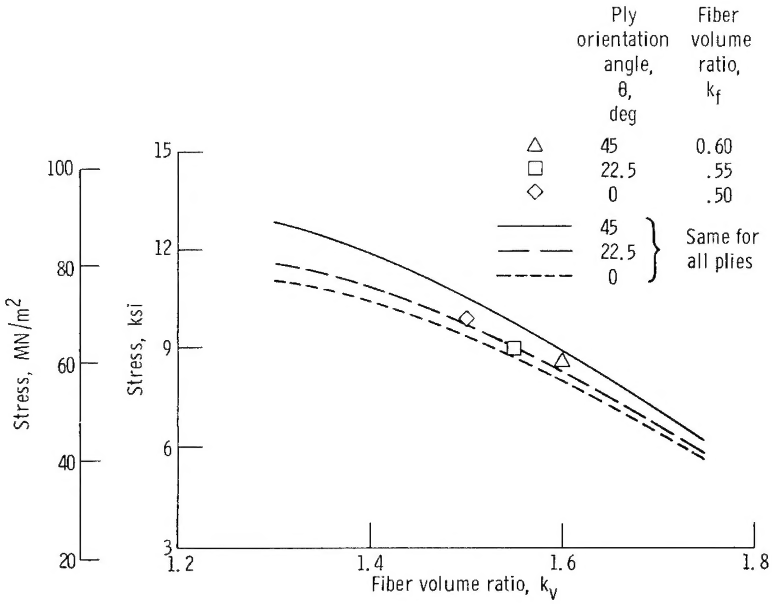

Figure 12. - Effect of having different groups of plies at different fiber contents on ply transverse residual stress. Modmor-I/polyimide composite; composite geometry, 24 [4(±45), 2(±22.5), 12(0), 2(∓22.5), 4(∓45)]; zero void content; temperature difference, 600° F (606 K).

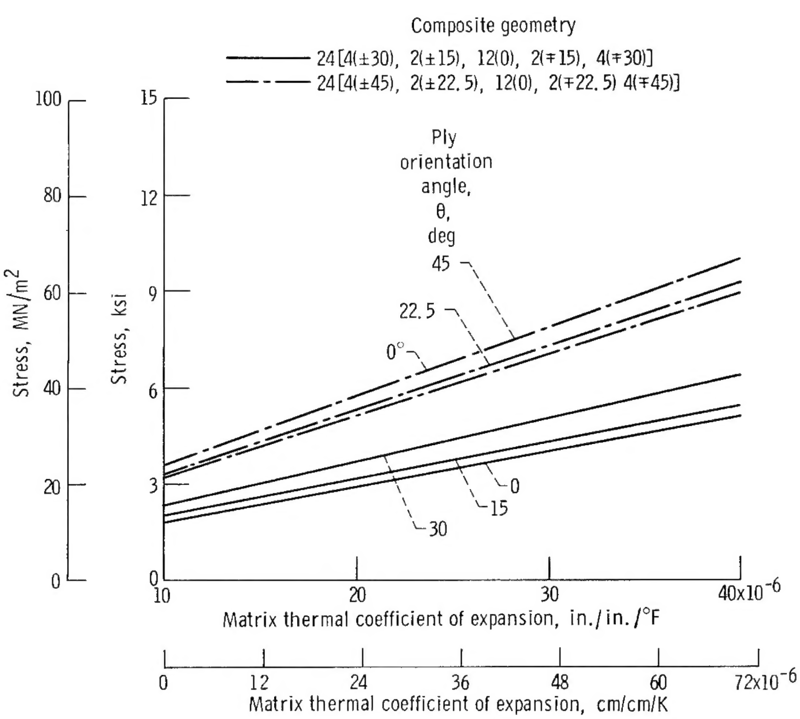

Figure 13. - Effects of matrix thermal coefficient of expansion on ply transverse residual stress. Modmor-I/polyimide composites; zero void content; fiber volume ratio, 0.50; temperature difference, 600° F (606 K).

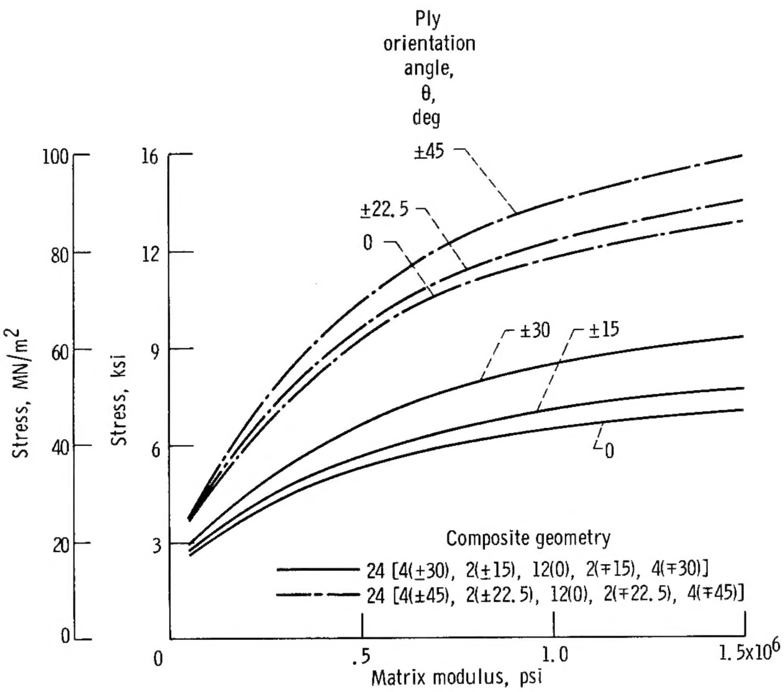

Figure 14. - Effect of matrix modulus on ply transverse residual stress. Modmor-I/polyimide composites; zero void content; fiber volume ratio, 0.50; temperature difference, 600° F (606 K).

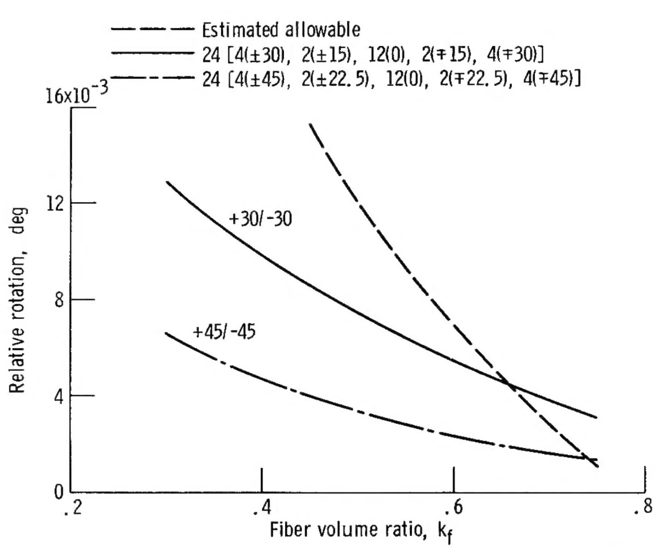

Figure 15. - Adjacent ply relative rotation due to residual stress for graphite Modmor-I/polyimide composites. Temperature difference, 600° F (606 K).

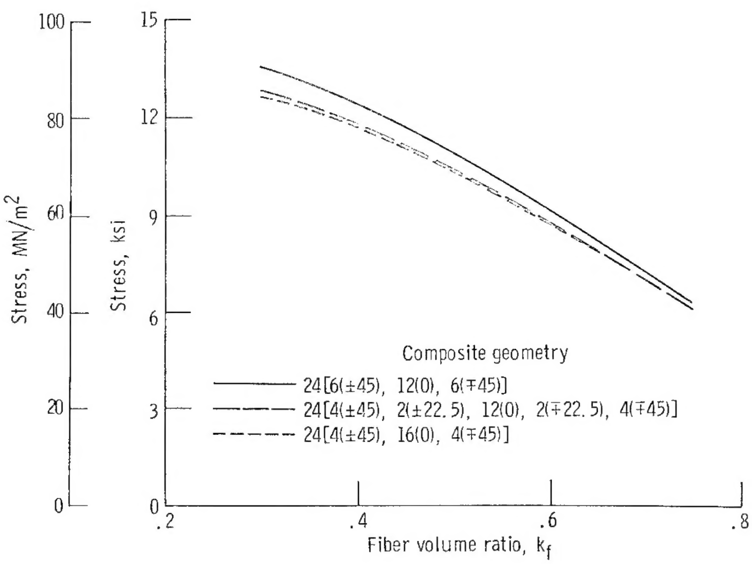

Figure 16. - Transitional plies and decreasing number of off-axis plies effect on ±45° ply residual transverse stress. Modmor-I/polyimide composite; temperature difference, 600° F (606 K).

NASA-Langley, 1971 —— 32 E-5848

NATIONAL AERONAUTICS AND SPACE ADMINISTRATION
WASHINGTON, D. C. 20546

OFFICIAL BUSINESS

FIRST CLASS MAIL

POSTAGE AND FEES PAI
NATIONAL AERONAUTICS
SPACE ADMINISTRATIO

06U 001 57 50 30S 71028 00942
PICATINNY ARSENAL
PLASTICS TECHNICAL EVALUATION CENTER
DOVER, NEW JERSEY 07801

ATT SMUPA-VP3

POSTMASTER: If Undeliverable (Section 1
Postal Manual) Do Not Re

"The aeronautical and space activities of the United States shall be conducted so as to contribute . . . to the expansion of human knowledge of phenomena in the atmosphere and space. The Administration shall provide for the widest practicable and appropriate dissemination of information concerning its activities and the results thereof."

— NATIONAL AERONAUTICS AND SPACE ACT OF 1958

NASA SCIENTIFIC AND TECHNICAL PUBLICATIONS

TECHNICAL REPORTS: Scientific and technical information considered important, complete, and a lasting contribution to existing knowledge.

TECHNICAL NOTES: Information less broad in scope but nevertheless of importance as a contribution to existing knowledge.

TECHNICAL MEMORANDUMS: Information receiving limited distribution because of preliminary data, security classification, or other reasons.

CONTRACTOR REPORTS: Scientific and technical information generated under a NASA contract or grant and considered an important contribution to existing knowledge.

TECHNICAL TRANSLATIONS: Information published in a foreign language considered to merit NASA distribution in English.

SPECIAL PUBLICATIONS: Information derived from or of value to NASA activities. Publications include conference proceedings, monographs, data compilations, handbooks, sourcebooks, and special bibliographies.

TECHNOLOGY UTILIZATION PUBLICATIONS: Information on technology used by NASA that may be of particular interest in commercial and other non-aerospace applications. Publications include Tech Briefs, Technology Utilization Reports and Technology Surveys.

Details on the availability of these publications may be obtained from:

SCIENTIFIC AND TECHNICAL INFORMATION OFFICE

NATIONAL AERONAUTICS AND SPACE ADMINISTRATION

Washington, D.C. 20546